Accounting for finite coherence in the analysis of dye sensitized solar cells and other thin film optoelectronic devices

Mayank Kumar Chaudhari*, Sachin Chaudhari**

*Department of Physics, Indian Institute of Technology (BHU), Varanasi
Uttar Pradesh - 221005, India

*Current affiliation: Faculty of Physical Sciences, INSH, SRM University, Lucknow
Uttar Pradesh - 225003, India

**Parul Institute of Engineering and Technology, Baroda
Gujarat - 391760, India

The optical properties of thin films are governed by coherent optics rather than geometrical optics. For this reason, various approaches based on coherent optics such as transfer matrix formulation are used extensively to study various thin film optoelectronic devices. Some thin film devices such as dye sensitized solar cells have layers which are thicker than the coherence length of light. Such a system having mixture of optically thin and optically thick media cannot be appropriately described either by coherent optics or ray optics alone. We formulate a framework based on coupled coherent and ray optics to account for finite coherence in modeling optical properties for thin film optoelectronics. We found that the optical response of the dye sensitized solar cell computed with coupled approach presented in this work shows better agreement with experimental results than that computed by transfer matrix formulation.

1. Introduction

Dye sensitized solar cells (DSCs) are explored extensively in past few decades [1–6]. The incredible research interest in DSCs is attributed mainly to their low cost, compatibility with flexible materials and ability to optimize different parts individually. Unlike semiconductor junction based solar cells, the basic processes namely light absorption, electron transport and hole transport is carried out by different materials in the DSCs thus giving flexibility to optimize each material separately for best performance [1]. Besides offering low cost advantage, thin film cells' flexibility and semitransparency makes them preferred choice for various applications such as window panes. Various challenges inherent in original design of dye sensitized solar cells such as liquid electrolyte which caused maintenance issues, need for strongly absorbing dyes and elimination of expensive components such as TCO and Pt coated electrodes are being addressed [7, 8]. Utilizing aforementioned flexibility in independent study of each component of DSCs researchers have explored and synthesized various dyes [9–11], various approaches have been proposed for improving efficiency of charge transport in TiO2 [12–15]. Approaches to enhance light harvesting efficiency (LHE) include photon confinement by brag reflectors and nano-tube structured TiO2 [16–20], use of diffuse scattering by introducing large-sized TiO2 particles [21,22] etc. The use of combined effect of scattering layer and photon confinement by Total Internal Reflections, later improved by use of directionally selective filters [23–25] have also been demonstrated both theoretically and practically by M. Peters et al.

The principle approaches used for theoretical study of thin film solar cells including DSCs are based on coherent optics model such as transfer matrix formulation [26, 27]. Computation of field intensity profiles, absorption depth profiles using transfer matrix formulation has been reported [27] and an approach to account for the parasitic absorptions in internal quantum efficiency measurements is proposed by Prof McGehee et al [22]. Yet the modeling of diffused scattering or radiative recombination processes in thin film structures is rather unexplored. We have formulated a method based on coupled coherent and geometrical approach to analyze effects of finite coherence on DSCs equipped with brag reflector. The study of interplay between coherent and geometrical optics governing the optical characteristics of layered media composed of thin films and the layers having thicknesses considerably greater than coherence length of incident light based on the approach presented herein can help explain the characteristics of layered media more accurately. Along with that it also provides a way to analyze characteristics of the thin films when under angularly selective filters such as Rugate filters on top of thick glass substrate. An efficient, highly flexible and robust approach based on combined coherent and geometrical optics has been presented here for precise modeling of DSCs and other thin film optoelectronic devices. This paper is organized in three sections. In the next section we describe the schematic model and the framework of the coupled approach in separate subsections and in the subsequent section of Results and Discussions we discuss the analysis of aforementioned DSCs and compare the results.

2. Coupled Coherent and Geometrical Optics Approach

The layered media comprising of optically thin layers (sufficiently thinner than coherence length of incident light) and optically thick layers, often encountered in thin film solar cells such as DSCs, can be modeled more accurately by first treating the identified thin films with coherent approach and then using the result to study the system as a whole with geometrical optics [28]. Layers such as glass substrates, electrolyte layer and sometimes the photo-anode in DSCs are typically much thicker than coherence length of sunlight and cannot be accurately modeled with coherent approach. Whereas the layers such as anti-reflective coating TCO and the layers comprising photonic crystal are much thinner and must be modeled with coherent approach to take into account the effects such as interference. In this section we first describe the theoretical model of DSCs and then explain the application of combined coherent and geometrical optics approach to analyze the model. In the next section we describe the results by comparing them with results obtained by transfer matrix approach and the practical results reported in the literature.

2.1. Modeling one-dimensional dye sensitized solar cell

We analyze the one-dimensional model of dye sensitized solar cell coupled with photonic crystal constructed by alternate layers of TiO2 and SiO2 repeated many times. Such models have been reported in literatures [26, 29–31]. The schematic diagram of the theoretical model and working of DSCs is shown in fig. 1. DSCs can typically be fabricated by printing porous TiO_2 nanoparticle film on transparent conducting oxide (TCO) coated glass substrate simply by applying the TiO_2 nanoparticle paste. Some advanced techniques include atomic layer deposition [32], pre-treatment of photoanode with $TiCl_4$ [33], preparation of thick inverse opals through a multi-cycle process [20] etc. The dye is anchored to the TiO_2-nanoparticle mesh by placing the printed glass substrate in dye solution for prolonged time. The cell is then sealed after placing adequate spacers and liquid I^-/I^{3-} redox pair based electrolyte is injected to completely drench the dye coated TiO_2 photo-electrode. One dimensional photonic crystal can be created by depositing SiO_2 and TiO_2 successively after the dye has been adsorbed on the photoanode [26]. The parameters affecting the optical properties of such layered media are wavelength dependent refractive indices, the thicknesses of each layer and the arrangement or the ordering of the layers. Thus for use in this model each layer is characterized by its thickness and the wavelength dependent complex refractive index.

2.2. Coupled coherent and geometric optics framework

Firstly, we identify the thin films and compute their reflection and transmission spectra by employing well-known transfer matrix formulation. For each layer transfer matrix can be formulated simply by applying suitable electromagnetic boundary conditions at the interfaces. The reflection and transmittance at the interface of two thick layers can be computed by Fresnel's equations. Now the thin films in the structures can be treated as interfaces with reflection and transmission properties computed by transfer matrix formulation. Note that in general reflectance and transmittance is not complementary for these interfaces as light is absorbed by thin films as well. At this point we are ready to treat the resultant model with geometrical optics. In other word we are coupling the output of coherent model to the geometrical optics model.

For easy and efficient implementation, we formulate an approach based on recursive or iterative algorithm. Just as we have computed reflection and transmittance spectra of thin films and then treated them as interface between two thick layers, we can even compute reflectance and transmission across a thick layer and then replace it by equivalent interface. The resulting system now is again a stack of thick layers, the input for next iteration. This kind of formulation allows us to use versatile iterative or recursive algorithm to compute optical properties of such layered media.

Firstly, the total transmission and reflectance across one layer for incidence from both the top and bottom side (reflectance and transmittance across a layer for incidence from opposite directions is not always same, e.g., when we are dealing with layers involving lossy dielectrics) are computed for one layer and then the layer is represented by equivalent interface having optical properties defined by following relations.

$$R_{11} = r_{11} + \frac{t_{11} r_{21} \exp(-2\alpha d) t_{12}}{1 - r_{12} r_{21} \exp(-2\alpha d)}$$

$$T_{11} = \frac{t_{11} \exp(-2\alpha d) t_{12}}{1 - r_{12} r_{21} \exp(-2\alpha d)}$$

Here, the first subscript is the index of the interface and second subscript denotes the direction. For example, the symbol r_{21} is used to represent the reflection coefficient of the 2nd interface when light is incident from the top and r_{12} is used to represent the reflection coefficient when light is incident on 1st interface from the bottom side. The symbols r and t represent the reflectance and transmittance of the interfaces whereas the capital symbols R and T represent the reflectance and transmittance of the layer as a whole respectively or in other words it represents the properties of the equivalent interface created by collapsing this layer. The coefficient of absorption is given by $\alpha = 4\pi Im(n)/\lambda$. Fig. 2 depicts multiple reflections and transmissions in the layered medium. The relations stated above can easily be derived by summing up intensities of individual reflections which is in the form of a geometric progression. Here it is worth mentioning that for geometrical optics considerations we simply add the intensities and thus account for absence of interference phenomena whereas in thin films the resultant is addition of amplitudes accounting for interference of electromagnetic waves reflected or transmitted by various interfaces in the system.

3. Results and Discussions

As discussed earlier, our approach is based on both coherent and geometrical optics formulation and thus it provides more accurate results compared to traditional transfer matrix approach. Firstly, we describe the analysis of the performance of DSCs equipped with a 1D Photonic Crystal in terms of its light harvesting efficiency. Secondly, we analyze the reflection and transmission characteristics of the cell. Thirdly, the electric field intensity distribution and finally, the photo-carrier generation rates in the device is analyzed.

We compare the results obtained in three different cases: 1. Using conventional transfer matrix method, i.e., whole cell is treated with coherent optics. 2. When some layers such as glass substrates and the electrolyte layers are considered thick layers and thus treated separately but the working electrode, where the light is actually harvested is treated as a part of the thin film. 3. When working electrode also is considered sufficiently thick so as to not allow sustainable interference and hence considered with geometrical optics. Comparison between fractions of light absorbed, reflected and transmitted and the photo-generation rate for a DSC under normal illumination for these three cases is shown in figure 3. For obtaining this results the DSC coupled to 1D photonic crystal and having anti-reflection coating of thickness 400 nm and refractive index 1.4 is considered. The complex refractive index of the working electrode is modeled by following equation.

$$n_{WE} = n_{TiO_2} + \beta . \exp(1 - \alpha - e^{\alpha})\, i,$$

$$where, \qquad \alpha = \frac{\lambda - \lambda_0}{d\lambda}$$

The thickness of working electrode is 1500 nm and the values of parameters defining refractive index of working electrode are $n_{TiO_2} = 1.95, \beta = 0.004, \lambda_0 = 538 nm\ and\ d\lambda = 64.16$. The photonic crystal is realized by alternating layers of TiO_2 and SiO_2 of refractive indices 1.92 and 1.43 and thicknesses 95nm and 80nm, respectively. The thickness and refractive indices of electrolyte and the glass substrate are $50\mu m$ and $30\mu m$, 1.433 and 1.6 respectively. It is evident from these results that finite coherence length has a significant effect on the optical properties and performance of the cell. Reflectance, transmittance and Light Harvesting Efficiency (LHE) are fluctuating very much with wavelength when the cell is treated with conventional transfer matrix method. The curves are smoother for the case when layers considerably thicker than working electrode are considered thick ones and treated accordingly. And the curves become very smooth for the case when working electrode also is considered thick layer. Thus, we will see different characteristics of the cell depending on the coherence length of the incident light. Since the sunlight has coherent length of approximately 8-10 wavelengths, the results corresponding to second case are most realistic for this cell under ordinary sunlight. Moreover, the difference in the performance is clearly seen in the photo-carrier generation rate profile. The electric field intensity profiles for selected wavelengths are shown in fig. 4. The cause of enhancement in LHE when DSC is coupled to 1D PC is evident from the localization effect seen in the electric field profiles for the wavelengths that are relatively strongly absorbed.

Next we compare LHE and Reflectance of two DSCs with 7500 nm thick working electrode (thick working electrode) and 600 nm thick working electrode (thin working electrode) as shown in fig. 5. For DSC with 7500 nm thick working electrode all parameters are same as the DSC used for fig. 3 except the thickness of working electrode. For DSC with 600 nm thick working electrode, β is taken to be 0.0055 and n_{TiO2} is taken to be 1.92. Moreover, the thickness of SiO_2 layer is changes to 60 nm, while the thickness of TiO_2 is kept the same. We have deliberately used same parameters that are used by Gabriel Lozano in [26] in order to compare the experimental and theoretical results and thus explain the effect of finite coherence length of light. When comparing our simulated results with experimental and theoretical results reported by Gabriel Lozano in [26], we found that the experimental results for DSC having 600 nm thick working electrode agrees more closely with results obtained by treating working electrode as a part of thin film (case 2) whereas the experimental results for DSC with 7500 nm thick electrode agrees better with results obtained by treating working electrode as thick layers (case 3). This is because coherence length of light is of the order of 8 to 10 wavelengths in case of sunlight, which is obviously much higher than 600 nm and comparable to 7500 nm. Thus, the effect of interference after reflections and refractions from multiple surfaces will be seen for 600 nm thick working electrode whereas such interference effects will be missing for 7500 nm thick electrode.

Thus, in conclusion we have formulated an approach based on both coherent and geometrical optics, which we call 'coupled coherent and geometrical optics approach' and this approach provides reasonably accurate results compared to the conventional transfer matrix approach or geometrical optics alone. Along with this we have also computed electric field intensity profile and absorption depth profile which could be used to explain the origin of enhancement in light harvesting by using 1D PC and as a input for electric model of the DSC.

References

1. B. E. Hardin, H. J. Snaith, and M. D. McGehee, "The renaissance of dye-sensitized solar cells," Nat. Photon-, vol. 6, pp. 162–169, 2012.
2. W. Tan, J. Chen, X. Zhou, J. Zhang, Y. Lin, X. Li, and X. Xiao, "Preparation of nanocrystalline TiO2 thin film at low temperature and its application in dye-sensitized solar cell," vol. 13, no. 5. SpringerVerlag, 01-May-2009.
3. J. Chen, F.-Q. Bai, J. Wang, L. Hao, Z.-F. Xie, Q.-J. Pan, and H.-X. Zhang, "Theoretical studies on spectroscopic properties of ruthenium sensitizers absorbed to TiO2 film surface with connection mode for DSSC," Dyes Pigment., vol. 94, pp. 459–468, Sep. 2012.
4. L. Ke, S. B. Dolmanan, L. Shen, P. K. Pallathadk, Z. Zhang, D. M. Y. Lai, and H. Liu, "Degradation mechanism of ZnO-based dye-sensitized solar cells," Sol. Energy Mater. Sol. Cells, vol. 94, pp. 323–326, Feb. 2010.
5. L. Jin, J. Zhai, L. Heng, T. Wei, L. Wen, L. Jiang, X. Zhao, and X. Zhang, "Bio-inspired multi-scale structures in dye-sensitized solar cell," J. Photochem. Photobiol. C: Photochem. Rev., vol. 10, pp. 149–158, 2009.
6. L. Kavan, N. Tétreault, T. Moehl, and M. Grätzel, "Electrochemical Characterization of TiO 2 Blocking Layers for Dye-Sensitized Solar Cells," J. Phys. Chem. C, vol. 118, pp. 16408–16418, Jul. 2014.
7. Q. Dai, D. R. MacFarlane, P. C. Howlett, and M. Forsyth, "Rapid I?/I3?: Diffusion in a MolecularPlastic-Crystal Electrolyte for Potential Application in Solid-State Photoelectrochemical Cells," Angew. Chem., vol. 117, pp. 317–320, Jan. 2005.
8. A. Mishra, M. K. R. Fischer, and P. Bäuerle, "Metal-free organic dyes for dye-sensitized solar cells: from structure: property relationships to design rules.," Angew. Chem., vol. 48, no. 14, pp. 2474–2499, 2009.
9. S. Mathew, A. Yella, P. Gao, R. Humphry-Baker, B. F. E. Curchod, N. Ashari-Astani, I. Tavernelli, U. Rothlisberger, M. K. Nazeeruddin, and M. Grätzel, "Dye-sensitized solar cells with 13% efficiency achieved through the molecular engineering of porphyrin sensitizers.," Nat. Chem., vol. 6, no. 3, pp. 242–247, 2014.
10. S. Ramkumar, S. Manoharan, and S. Anandan, "Synthesis of D-($\uppi$-A)2 organic chromophores for dye-sensitized solar cells," Dyes Pigment., vol. 94, pp. 503–511, Sep. 2012.
11. J.-J. Cid, J.-H. Yum, S.-R. Jang, M. K. Nazeeruddin, E. Martínez-Ferrero, E. Palomares, J. Ko, M. Grätzel, and T. Torres, "Molecular Cosensitization for Efficient Panchromatic Dye-Sensitized Solar Cells," Angew. Chem., vol. 119, pp. 8510–8514, Nov. 2007.
12. S. H. Ko, D. Lee, H. W. Kang, K. H. Nam, J. Y. Yeo, S. J. Hong, C. P. Grigoropoulos, and H. J. Sung, "Nanoforest of hydrothermally grown hierarchical ZnO nanowires for a high efficiency dyesensitized solar cell.," Nano Lett., vol. 11, no. 2, pp. 666–671, 2011.
13. J. Shen, R. Cheng, Y. Chen, X. Chen, Z. Sun, and S. Huang, "A Novel TiO_2 Tape for Fabricating Dye-Sensitized Solar Cells on Universal Conductive Substrates," ACS Appl. Mater. & Interfaces, vol. 5, no. 24, pp. 13000–13005, Dec. 2013.
14. K.-J. Jiang, J.-M. Zhou, K. Manseki, Q.-S. Liu, J.-H. Huang, Y. Song, and S. Yanagida, "Integration of High-Performance Nanocrystalline TiO 2 Photoelectrodes for N719-Sensitized Solar Cells," Int. J. Photoenergy, vol. 2013, pp. 1–6, 2013.
15. M. M. Khan, S. A. Ansari, D. Pradhan, M. O. Ansari, D. H. Han, J. Lee, and M. H. Cho, "Band gap engineered TiO 2 nanoparticles for visible light induced photoelectrochemical and photocatalytic studies," J. Mater. Chem., vol. 2, pp. 637–644, 2014.
16. M. Guo, Z. Yong, K. Xie, J. Lin, Y. Wang, and H. Huang, "Enhanced Light Harvesting in DyeSensitized Solar Cells Coupled with Titania Nanotube Photonic Crystals: A Theoretical Study," ACS Appl. Mater. & Interfaces, Dec. 2013.

17. M. R. Mohammadi, R. R. M. Louca, D. J. Fray, and M. E. Welland, “Dye-sensitized solar cells based on a single layer deposition of TiO2 from a new formulation paste and their photovoltaic performance,” Sol. Energy, vol. 86, pp. 2654–2664, Sep. 2012.
18. H. Wang, J. He, G. Boschloo, H. Lindström, A. Hagfeldt, and S.-E. Lindquist, “Electrochemical Investigation of Traps in a Nanostructured TiO_2 Film,” J. Phys. Chem. B, vol. 105, no. 13, pp. 2529–2533, Mar. 2001.
19. S. I. Cha, K. H. Hwang, Y. H. Kim, M. J. Yun, S. H. Seo, Y. J. Shin, J. H. Moon, and D. Y. Lee, “Crystal splitting and enhanced photocatalytic behavior of TiO2 rutile nano-belts induced by dislocations,” Nanoscale, vol. 5, no. 2, pp. 753–758, Dec. 2012.
20. C.-Y. Kuo and S.-Y. Lu, “Fabrication of a multi-scale nanostructure of TiO2 for application in dyesensitized solar cells,” Nanotechnology, vol. 19, 2008.
21. M. Patterson, S. Hughes, S. Combri’e, N.-V.-Q. Tran, A. D. Rossi, R. Gabet, and Y. Jaouen, “Disorder-induced coherent scattering in slow-light photonic crystal waveguides,” arXiv ePrints, Jun. 2009.
22. G. F. Burkhard, E. T. Hoke, and M. D. McGehee, “Accounting for interference, scattering, and electrode absorption to make accurate internal quantum efficiency measurements in organic and other thin solar cells.,” Adv. Mater., vol. 22, no. 30, pp. 3293–3297, 2010.
23. M. Peters, J. C. Goldschmidt, T. Kirchartz, and B. Bläsi, “The photonic light trap—Improved light trapping in solar cells by angularly selective filters,” Sol. Energy Mater. Sol. Cells, vol. 93, pp. 1721–1727, Oct. 2009.
24. M. Peters, J. C. Goldschmidt, and B. Bläsi, “Angular confinement and concentration in photovoltaic converters,” Sol. Energy Mater. Sol. Cells, vol. 94, pp. 1393–1398, Aug. 2010.
25. M. Peters, C. Ulbrich, J. C. Goldschmidt, J. Fernandez, G. Siefer, and B. Bläsi, “Directionally selective light trapping in a germanium solar cell,” Opt. Express, vol. 19. Optical Society of America (OSA), p. 136, 2011.
26. G. Lozano, S. Colodrero, O. Caulier, M. E. Calvo, and H. Mi´guez, “Theoretical Analysis of the Performance of One-Dimensional Photonic Crystal-Based Dye-Sensitized Solar Cells,” J. Phys. Chem. C, vol. 114, pp. 3681–3687, Mar. 2010.
27. L. A. A. Pettersson, L. S. Roman, and O. Inganäs, “Modeling photocurrent action spectra of photovoltaic devices based on organic thin films,” J. Appl. Phys., vol. 86, 1999.
28. S. Wenger, M. Schmid, G. Rothenberger, A. Gentsch, M. Grätzel, and J. O. Schumacher, “Coupled Optical and Electronic Modeling of Dye-Sensitized Solar Cells for Steady-State Parameter Extraction,” J. Phys. Chem. C, vol. 115, pp. 10218–10229, May 2011.
29. A. Mihi and H. Míguez, “Origin of Light-Harvesting Enhancement in Colloidal-Photonic-CrystalBased Dye-Sensitized Solar Cells,” J. Phys. Chem. B, vol. 109, pp. 15968–15976, Aug. 2005.
30. S. Colodrero, A. Mihi, J. A. Anta, M. O. a, and H. Míguez, “Experimental Demonstration of the Mechanism of Light Harvesting Enhancement in Photonic-Crystal-Based Dye-Sensitized Solar Cells,” J. Phys. Chem. C, vol. 113, pp. 1150–1154, Jan. 2009.
31. S. Colodrero, A. Mihi, L. Häggman, M. Ocaña, G. Boschloo, A. Hagfeldt, and H. Míguez, “Porous One-Dimensional Photonic Crystals Improve the Power-Conversion Efficiency of Dye-Sensitized Solar Cells,” Adv. Mater., vol. 21, pp. 764–770, Feb. 2009.
32. D. Hess, M. Mushfiq, R. Dalvi, R. Winter, U. Sampathkumaran, K. Goswami, A. Yangaus-Gil, and J. W. Elam, “Dye-Sensitized Solar Cells Fabricated from Atomic Layer Deposited Photoanodes on Aerogel Scaffolds.”
33. S. Ito, T. N. Murakami, P. Comte, P. Liska, C. Grätzel, M. K. Nazeeruddin, and M. Grätzel, “Fabrication of thin film dye sensitized solar cells with solar to electric power conversion efficiency over 10%,” Thin Solid Films, vol. 516, pp. 4613–4619, May 2008.

Figure Captions

1. Schematic diagram of construction and working of a DSC.
2. Multiple reflections and transmissions within layered medium.
3. Absorption spectrum (a), reflectance spectrum (b), photo-carrier generation rate as a function of position in the device (c) for a DSC when under normal incidence, Light gray lines, thin black line and dark (thick) black line is used for results corresponding to cases 1, 2 and 3 as described in the text respectively.
4. Electric field intensity profiles for selected wavelengths in the region of working electrode and photonic crystal. Light gray, blue and red lines are used for results corresponding to cases 1, 2 and 3 as described in the text respectively.
5. Comparison between LHE and Reflectance for DSC having 600 nm thick working electrode (top) and DSC having 7500 nm thick working electrode (bottom). Results corresponding to case 2 are expected to be in greater agreement with the experimental results for 600nm thick working electrode and thus are shown by dark black line. Whereas for 7500 nm thick working electrode the results corresponding to case 3 are expected to be in greater agreement with experimental results using ordinary sunlight and thus are shown by dark black line.

Figures:

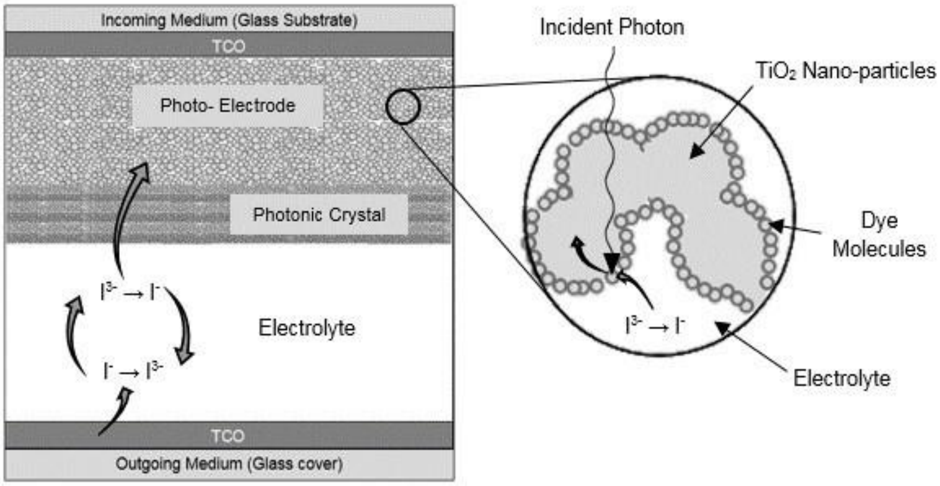

Fig. 1

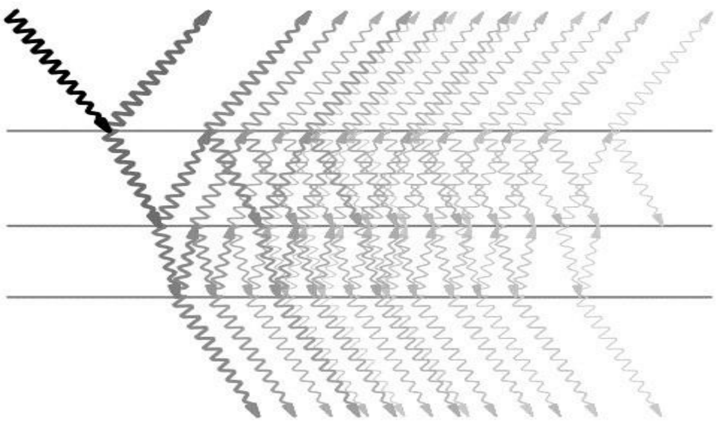

Fig. 2

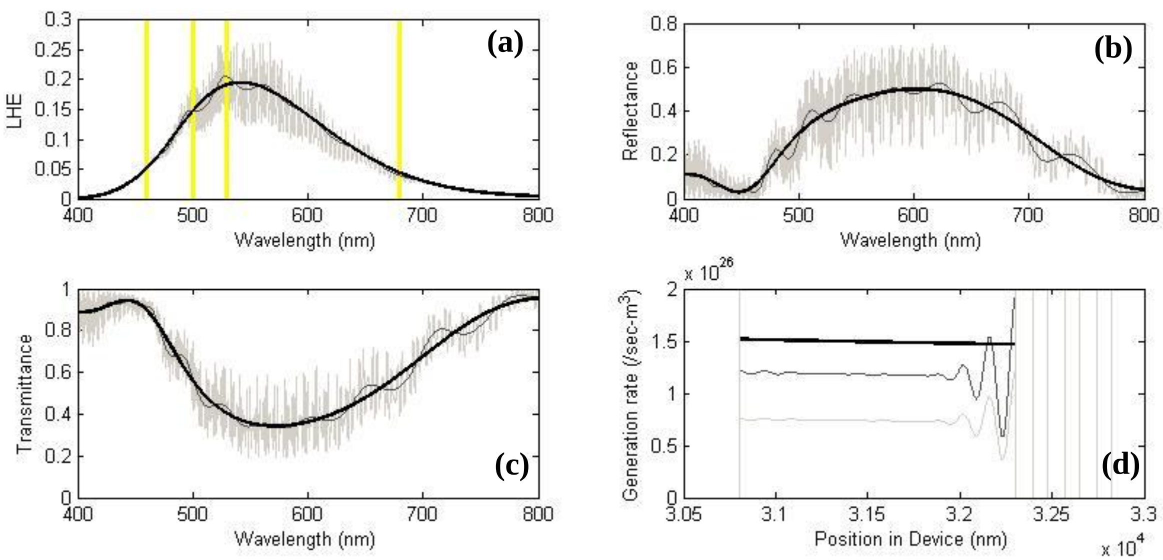

Fig.3

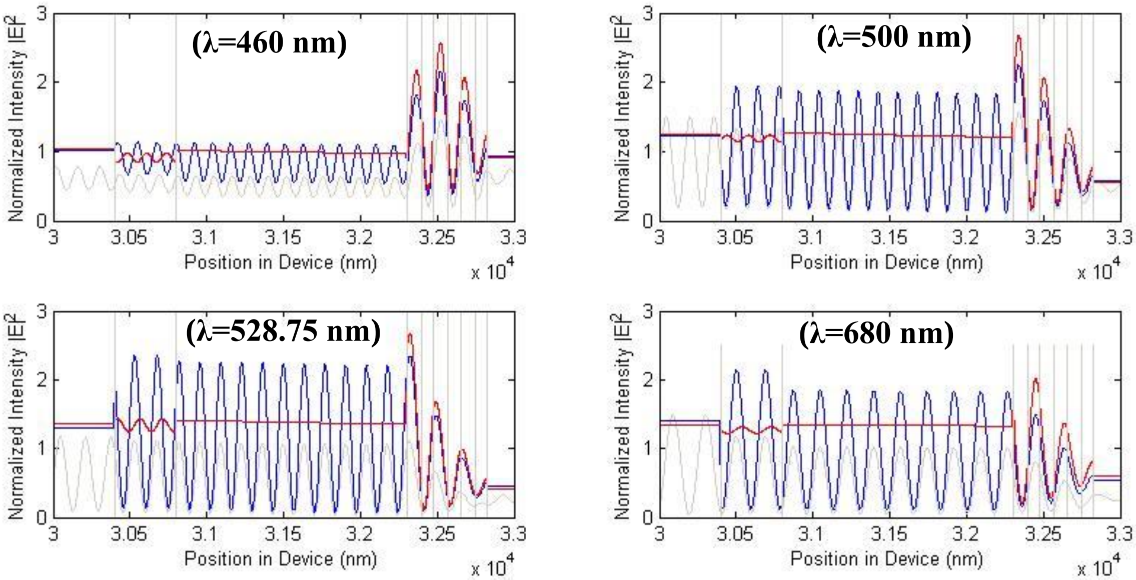
(λ=460 nm)
(λ=500 nm)
(λ=528.75 nm)
(λ=680 nm)
Normalized Intensity |E|2
Position in Device (nm)
x 10^4

Fig. 4

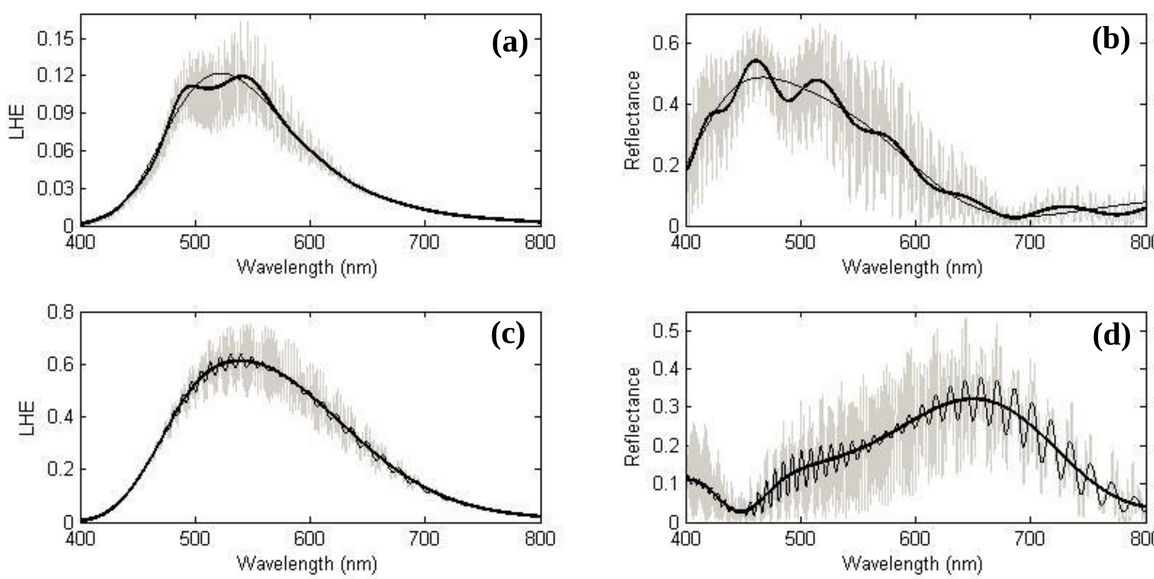
(a)
(b)
(c)
(d)
LHE
Reflectance
Wavelength (nm)

Fig. 5